

Selective oxidation of methane to syngas over NiO/barium hexaaluminate

Wenling Chu*, Weishen Yang and Liwu Lin

State Key Laboratory of Catalysis, Dalian Institute of Chemical Physics, Chinese Academy of Sciences, PO Box 110, Dalian 116023, PR China
E-mail: wlchu@online.ln.cn

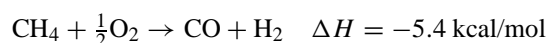
Received 18 January 2001; accepted 12 April 2001

The preparation, characterization and reactivity of NiO over barium hexaaluminate in the partial oxidation of methane is investigated. It is found that the prepared NiO supported catalysts are extremely active in the catalytic oxidation of methane, with 95% CH₄ conversion and 98% CO selectivity achieved at 850 °C. Highly disperse nickel oxide interacting with the support clearly shows the efficient use of the active nickel phase. In particular, the special structure of the barium hexaaluminate prevents its lattice from being destroyed by Ni ions when the Ni loading is as high as 20 wt%. The “layered aluminate type” structure of the barium hexaaluminate support can accommodate Ni ions in the structure so that there exists interaction between Ni ions and support, which causes the supported catalysts to possess excellent stability and capability to suppress carbon deposition.

KEY WORDS: partial oxidation of methane; barium hexaaluminate; nickel catalyst; carbon deposition

1. Introduction

Catalytic partial oxidation of methane to CO and H₂



has attracted a considerable interest in the last ten years [1–4] for the chemical utilization of natural gas. Unlike the methane steam reforming [5,6], which suffers from limitations, such as very high energy requirements, high H₂/CO product ratio (which is not suitable for Fischer–Tropsch synthesis) and poor selectivity for CO, the partial oxidation of methane is not at all energy intensive, and therefore, it is of great practical importance. It was found that nickel-based catalysts emerge as the most practical option because of their high activity and low cost [7]. But Ni-based catalysts were found to be deactivated more easily due to sintering of both the active metal and the support oxide [8,9], the deposition of carbon [10,11] as well as the sintering and loss of the active metal [12,13]. Maintaining the stability and activity of the catalyst against sintering and coke formation is one of the most important considerations before this process can be used on an industrial scale.

Alumina is widely used as an oxide support, but its surface area significantly decreases with the transition from metastable phase into the α -phase [14]. Although the surface area of the support does not directly affect the activity of the methane oxidation, a high surface area is desired to maintain high dispersion of catalytic components. It is well known that the deactivation of alumina-supported catalysts during high-temperature reaction is linked to the thermal deterioration of the alumina support, which causes sintering and leads to pore closing and reduction in surface area as well as

phase transformation into α -Al₂O₃, which changes the active surface layer and promotes a low surface area structure. Preventing the alumina support from thermal deterioration has been studied by many authors [15,16], but few materials satisfy both high heat resistance and large surface area at the temperature of interest.

Some researchers have greatly enhanced the catalytic activity and stability of Ni catalysts by adding a large number of additives to the alumina support to inhibit sintering and phase transformation. Additive basic oxides, such as CaO, MgO, La₂O₃, BaO [3,17,18], *etc.*, have been reported to aid in maintaining catalytic activity and suppressing the deactivation, owing to the interaction between NiO and supports. Here, we used barium hexaaluminate (BaO·6Al₂O₃) with high thermal stability and high surface area as the support material. Owing to the formation of a hexaaluminate phase, barium hexaaluminate exhibited excellent heat resistance against sintering at high temperature. This material retained a surface area near 10 m²/g after 5 h of calcination at 1600 °C, and this large surface area can be always retained when the hexaaluminate structure is formed.

The present investigation was undertaken to study the oxidative methane to syngas conversion over NiO supported on the barium hexaaluminate. An attempt is made to develop a supported catalyst with high thermal stability against sintering and excellent ability to suppress carbon deposition.

2. Experimental

2.1. The preparation of the support and catalyst

Here, we used a simple preparation method to synthesize the barium hexaaluminate support [19]. First, a clear solu-

* To whom correspondence should be addressed.

tion was obtained by dissolving $\text{Ba}(\text{NO}_3)_2$ in hot deionized water, then acidifying to $\text{pH} \approx 1$ with HNO_3 , and finally adding $\text{Al}(\text{NO}_3)_3 \cdot 9\text{H}_2\text{O}$. This solution was poured under vigorous stirring in a $(\text{NH}_4)_2\text{CO}_3$ solution in large excess, heated at 60°C . During the precipitation, the pH remained constant at 7.5–8.0. The slurry was then aged for several hours at 60°C and filtered. The filter cake was washed to remove nitrates and then dried at 110°C overnight in air. The powders thus obtained were calcined at different temperatures for 5 h.

The supported catalyst was prepared by impregnating barium hexaaluminate with nickel acetate solution. The loading of supported nickel ranged from 0.5 to 20 wt% Ni. The resulting materials were then dried and calcined in air for 5 h at 800°C .

2.2. The characterization of the support and catalyst

X-ray diffraction (XRD) analysis was performed by using a Rigaku D-Max/RB with $\text{Cu K}\alpha$ radiation. The samples were measured with a 2θ scan from 10° to 80° with scanning rate of $8^\circ/\text{min}$.

Fourier transform infrared (FT-IR) spectra were recorded on a Nicolet Impact 410 spectrophotometer, using the KBr pressed disk technique.

Surface area measurements were performed with a Coulter Omnisorp 100CX using BET nitrogen absorption.

Fresh and used catalysts have been characterized for their surface properties using X-ray photoelectron spectroscopy (XPS). XPS spectra were recorded using a VG ESCALAB MK-2X spectrometer, equipped with a single channel detector with $\text{Al K}\alpha$ radiation. The C_{1s} peak at 284.6 eV due to adventitious carbon was used as an internal standard for NiO, the Al_{2p} peak at 74.7 eV was used as an internal standard for all $\text{BaO} \cdot 6\text{Al}_2\text{O}_3$ -supported samples.

The reduction properties of samples were measured by means of temperature-programmed reduction (H_2 -TPR). The weight of the sample is 100 mg in this work. The samples were pre-treated in a flow of Ar at a heating rate of $10^\circ\text{C}/\text{min}$ up to 700°C , and subsequently in an Ar flow at 700°C for 1 h. After cooling in the protection of Ar to 50°C , the feed gas was simultaneously switched to 5% H_2 -Ar mixture until the base line is not changed. Then the temperature was increased from 50 to 1050°C at a rate of $10^\circ\text{C}/\text{min}$. A thermal conductivity detector (TCD) was used on line for signal detection.

2.3. Catalytic oxidation of methane

Catalytic activities were tested in a fixed-bed apparatus using a quartz reactor at atmospheric pressure. The catalysts were pre-reduced in H_2/He mixture flow for 1 h at 850°C before testing. Helium was used as a diluent (40 vol%). The standard reaction conditions were: reaction temperature range 500 – 950°C , $\text{CH}_4/\text{O}_2 = 2/1$, $F/W = 1.2 \times 10^4 \text{ ml/g h}$, the amount of catalysts 0.5 g. The reaction products were analyzed using a HP 6890 gas chromatograph equipped with

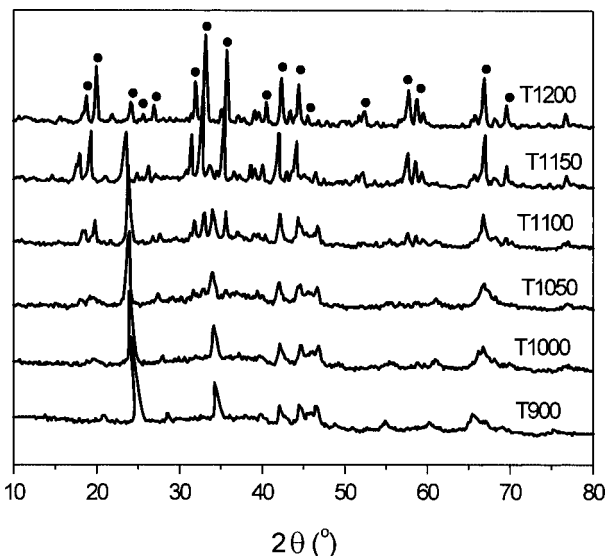


Figure 1. X-ray diffraction patterns of the $\text{BaO}-\text{Al}_2\text{O}_3$ support system after calcination at various temperatures. (●) $\text{BaO} \cdot 6\text{Al}_2\text{O}_3$.

Table 1
Calcination temperature dependence of the surface area of the $\text{BaO}-\text{Al}_2\text{O}_3$ support system.

	Calcination temp. ($^\circ\text{C}$)					
	900	1000	1050	1100	1150	1200
Surface area (m^2/g)	143.5	125.3	96.5	88.1	48.6	17.7

an automatic sampling valve and a TCD detector. Two columns Porapak Q and 5A sieve were used in a series/by pass arrangement for the complete separation of CH_4 , CO_2 , H_2 , O_2 and CO . An ice bath was set between the reactor exit and the GC sampling valve to remove the water.

3. Results and discussion

3.1. The characteristics of the $\text{BaO} \cdot 6\text{Al}_2\text{O}_3$ support

The X-ray diffraction patterns of the $\text{BaO}-\text{Al}_2\text{O}_3$ support system after calcination at various temperatures can be observed in figure 1. It is noted that the samples calcined below 1050°C should be mixtures of alumina phase and $\text{BaO} \cdot \text{Al}_2\text{O}_3$ (which is produced from γ -alumina and barium carbonate), whereas the diffraction lines from $\text{BaO} \cdot 6\text{Al}_2\text{O}_3$ phase are too weak to be observed due to its poor crystallinity. With a rise in calcination temperature, the diffraction lines from $\text{BaO} \cdot 6\text{Al}_2\text{O}_3$ appeared and became intense (completed at 1200°C for 5 h), and despite the high calcination temperature, no formation of sintered alumina phase such as θ - or α - Al_2O_3 is detected. However, for traditional γ - Al_2O_3 supports, phase transformation, which results in sintering or grain growth, occurred in the following sequence with increasing temperature, $\gamma \rightarrow \delta \rightarrow \theta \rightarrow \alpha$ [20]. At 1200°C , the sample shows a surface area of $17.7 \text{ m}^2/\text{g}$ (see table 1), which is about four times higher than that of pure γ -alumina [21]. A progressive but slow

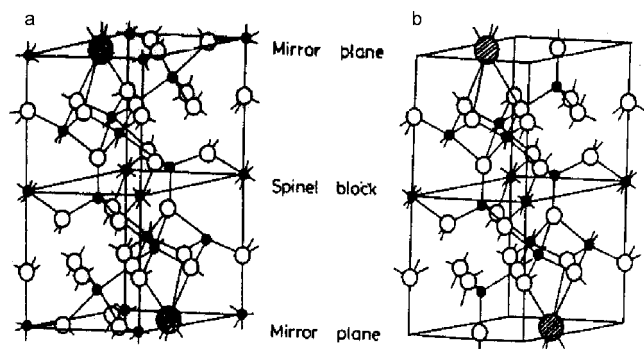


Figure 2. Crystal structures of (a) magnetoplumbite and (b) β -alumina. (●) Al^{3+} , (○) O^{2-} and (●) Ba^{2+} .

decrease in the surface area values is observed with increasing calcination temperature; after calcination at 1100°C , surface area decreases to $88.1\text{ m}^2/\text{g}$. Upon calcination at 1200°C , a marked drop in surface area value is observed associated with the formation of the final $\text{BaO}\cdot 6\text{Al}_2\text{O}_3$ phase. No changes in the phase composition and in the surface area of the sample are measured after calcination up to 1300°C for 10 h in line with the literature data [22]. It suggests that barium hexaaluminate, as a support material, possesses high structure stability against sintering and potential application for industry.

Not enough FT-IR spectra of the $\text{BaO}\text{--}\text{Al}_2\text{O}_3$ support system further confirmed the formation of $\text{BaO}\cdot 6\text{Al}_2\text{O}_3$ phase, as observed from XRD. With lower calcination temperature, the broad bands observed near 600 and 800 cm^{-1} are indicative of the disorder in the cation distribution in the defective spinel-type phase of $\gamma\text{-Al}_2\text{O}_3$. On increasing the calcination temperature to 1150°C , the characteristic peaks of $\text{BaO}\cdot 6\text{Al}_2\text{O}_3$ with sharp maxima at $586, 623, 653, 685, 750$ and 860 cm^{-1} were observed, which are the same as those reported by Busca [23,24] and Bellotto [25] according to their IR results.

From the results above, we can conclude that the formation of $\text{BaO}\cdot 6\text{Al}_2\text{O}_3$ may play a key role in maintaining the excellent heat resistance and high surface area. Many researchers ascribed such high thermal resistance against sintering and high surface area to the special structure of $\text{BaO}\cdot 6\text{Al}_2\text{O}_3$ [26,27]. It was reported that the structure of $\text{BaO}\cdot 6\text{Al}_2\text{O}_3$ is an intermediate of two types of related aluminate shown in figure 2. Both the magnetoplumbite and β -alumina structures are grouped into a layered alumina type, but they differ from each other in the atomic arrangement in the mirror plane. It is the layered alumina structure separated by the mirror plane that appears to suppress interlayer diffusion of atoms and crystal growth and exhibited a large surface area after heating at high temperature, which seems to play an important role in high-temperature catalytic reaction.

3.2. The partial oxidation of methane over $\text{NiO}/\text{BaO}\cdot 6\text{Al}_2\text{O}_3$

We examined the catalytic activity of the partial oxidation of methane over the reduced $\text{NiO}/\text{BaO}\cdot 6\text{Al}_2\text{O}_3$ cata-

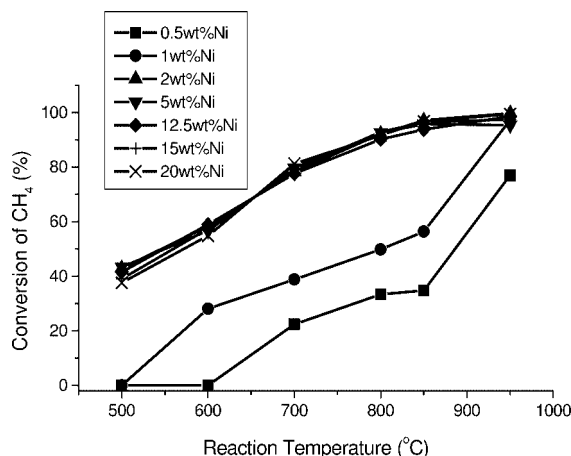


Figure 3. Effect of reaction temperature on conversion of CH_4 over $\text{NiO}/\text{BaO}\cdot 6\text{Al}_2\text{O}_3$ catalyst with variable Ni loading ($\text{CH}_4/\text{O}_2/\text{He} = 2/1/2$, GHSV = 12000 ml/g h).

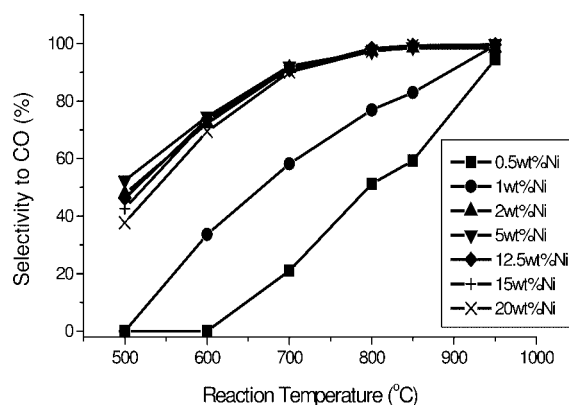


Figure 4. Effect of reaction temperature on selectivity to CO over $\text{NiO}/\text{BaO}\cdot 6\text{Al}_2\text{O}_3$ catalyst with variable Ni loading ($\text{CH}_4/\text{O}_2/\text{He} = 2/1/2$, GHSV = 12000 ml/g h).

lysts under atmospheric pressure. Neither pure NiO nor $\text{BaO}\cdot 6\text{Al}_2\text{O}_3$ support showed appreciable activity for the methane oxidation at 850°C . However, supported $\text{NiO}/\text{BaO}\cdot 6\text{Al}_2\text{O}_3$ catalysts are significantly active for this reaction. The differences in activities may be related to the interaction between NiO and support. The catalytic activities of the reduced supported catalysts for the reaction in the temperature range between 500 and 950°C are shown in figures 3 and 4. The products were CO , CO_2 , H_2O and H_2 ; no C_2 products were detected. The oxygen conversion was almost complete at all reaction temperatures $\geq 500^\circ\text{C}$. Both the conversion of CH_4 and selectivity to CO rapidly increased with increase in the reaction temperature, and 95% of conversion and 98% of selectivity were reached at 850°C , which is slightly higher than the activity of alumina-supported nickel catalyst ($\text{NiO}/\text{Al}_2\text{O}_3$). 88% of the maximum conversion with 92% of selectivity was obtained for 12.5 wt% Ni loading with equivalent pretreatment and reaction conditions.

The effect of Ni loading on the catalytic properties at 850°C was also examined. It was found that the activity and CO selectivity increase rapidly with increasing Ni loading

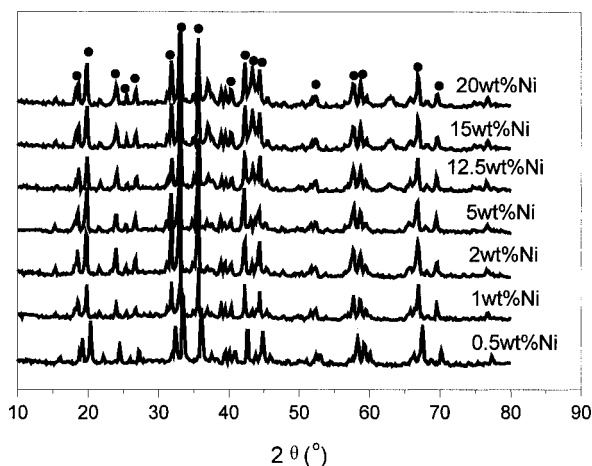


Figure 5. X-ray diffraction patterns of NiO/BaO-6Al₂O₃ with various Ni loadings. (•) BaO·6Al₂O₃.

when the Ni loading is lower than 2 wt%. When the Ni loading exceeds 2 wt%, there is little additional change in either activity or CO selectivity with increasing Ni loading, and conversion of CH₄ and selectivity to CO remained 95 and 98%, respectively. This phenomenon is contrary to the traditional opinion, in which the activity of the catalysts present a maximum with increasing loading, and the activity of the catalyst with high loading is often very low, either due to decomposition of the support structure by active species dispersed into the lattice of the support during calcination [28] or due to the crystallization of the active species [29]. As shown in figure 5, XRD spectra showed that no crystallized NiO species was detected even with Ni loading as high as 20 wt%, suggesting that NiO is highly dispersed into the BaO·6Al₂O₃ lattice, where NiO no longer exists in a crystalline state. It was also shown by XRD that the support retains its characteristic structure and that high Ni loadings do not lead to detectable decomposition of the support lattice. It is suggested that the special “layered aluminate structure” of BaO·6Al₂O₃ may play an important role in maintaining the stability. According to the results reported earlier [30], the replacement of Al³⁺ by Ni²⁺ is allowed by a charge compensation mechanism which can operate due to the presence of cation vacancies in the mirror planes of the structure [31]. This indicates that the BaO·6Al₂O₃ phase can accommodate foreign Ni ions in the structure replacing the Al³⁺ cations in both the tetrahedral and octahedral coordination [22], but the substitution of Ni ions into the lattice of the BaO·6Al₂O₃ support does not lead to the decomposition of its structure. As such it is believed that the high activity of the high Ni loading catalyst is due to the special structure stability of the BaO·6Al₂O₃ support.

TPR measurements further support this interpretation. Figure 6 illustrates the TPR profile of the catalysts. BaO·6Al₂O₃ support did not show a reduction peak up to 1050 °C. The TPR measurement of pure NiO showed a reduction profile between 300 and 500 °C centered at 400 °C, which has been explained in the literature as the reduction of NiO to Ni [32,33]. The TPR profiles of the supported cat-

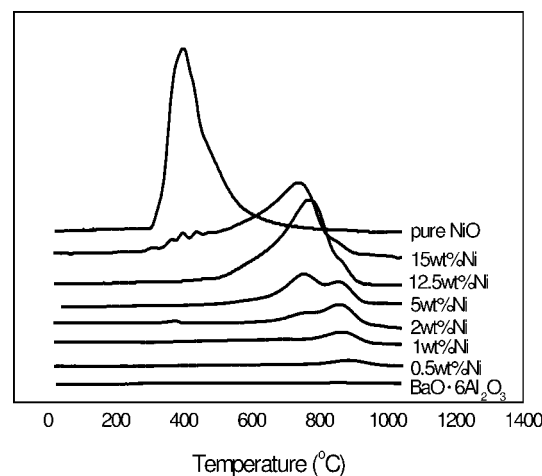


Figure 6. The H₂-TPR profiles of pure NiO, BaO·6Al₂O₃ support and NiO/BaO·6Al₂O₃ with various Ni loadings.

alysts indicates that the reduction peak of NiO disappeared, meaning that there is no single NiO species on the surface of the support, as confirmed by the XRD results (figure 5). It implies that Ni ions reacted with BaO·6Al₂O₃ support and are incorporated into its structure. The presence of peaks at much higher reduction temperature, starting to be reduced at about 800 °C, indicates that Ni cations are strongly stabilized. Scheffer *et al.* [34] identified different nickel species in an alumina-supported catalyst, based on the temperature range in which the species were reduced:

- up to 400 °C: reduction of bulk nickel oxide;
- 400–750 °C: reduction of disperse nickel oxide interacting with the support;
- 750–1000 °C: reduction of nickel aluminates.

For the catalysts with lower Ni loadings (<2 wt%), one reduction peak at 870 °C in the TPR profiles indicates the presence of aluminate compounds formed by the stronger interaction between the nickel and support. However, the catalysts with 2 and 5 wt% Ni content show two hydrogen consumption peaks, at 750 and 870 °C, respectively, meaning that a second highly nickel species appeared. Appearance of this species is an important feature of the studied catalysts since it may be catalytically active for the partial oxidation of methane. This conclusion is supported by the activity results discussed above, which indicates that increasing Ni loading to 2 wt% resulted in a sudden increase in both activity and selectivity. With further increase in Ni loading ≥12.5 wt%, the TPR peak of nickel aluminates was observed as a large peak at ~750 °C which may be attributed to the reduction of disperse nickel oxide, the presence of which clearly shows the efficient use of the active nickel phase, making the catalysts industrially attractive.

According to XPS results, we can support the same interpretation as from the TPR data. Table 2 displays the data of the binding energy in O_{1s}, Ni_{2p_{3/2}} and Ni_{2p_{1/2}} regions for the catalysts. It has been reported in [35] that the binding energies of O_{1s}, Ni_{2p_{3/2}} and Ni_{2p_{1/2}} for pure NiO are 529.9,

Table 2
XPS binding energies in O_{1s} and Ni_{2p} regions.

Sample	Binding energy (eV)			
	O _{1s}	Ni _{2p_{3/2}}	Ni _{2p_{1/2}}	Al _{2p}
NiO	528.8	852.8	871.3	–
0.5 wt% NiO/BaO·6Al ₂ O ₃	531.2	855.7	873.1	74.7
1 wt% NiO/BaO·6Al ₂ O ₃	531.2	855.6	873.2	74.7
2 wt% NiO/BaO·6Al ₂ O ₃	531.2	855.4	873.4	74.7
5 wt% NiO/BaO·6Al ₂ O ₃	531.2	855.4	872.9	74.7
12.5 wt% NiO/BaO·6Al ₂ O ₃	531.3	855.2	872.4	74.7
15 wt% NiO/BaO·6Al ₂ O ₃	531.1	855.0	872.7	74.7
20 wt% NiO/BaO·6Al ₂ O ₃	531.3	855.0	872.8	74.7

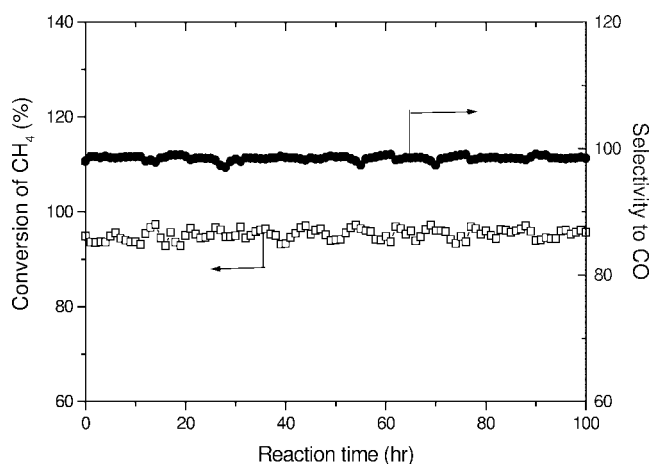


Figure 7. Influence of time-on-stream (GHSV = 12000 ml/g h) on the conversion of methane and selectivity to CO over NiO/BaO·6Al₂O₃ (5 wt% Ni loading) at 850 °C.

854.0 and 872.4 eV, respectively, and relative binding energies for pure NiAl₂O₄ are 531.3, 856.1 and 873.8 eV, respectively. The resulting XPS spectra (table 2) revealed that NiO phase was absent on the supported samples, which consisted primarily of the dispersed nickel oxide interacting with the support (higher Ni loading) and NiAl₂O₄ phase (lower Ni loading).

The effect of time on stream, up to 100 h, is presented in figure 7 for the 5 wt% NiO/BaO·6Al₂O₃ catalyst at 850 °C. As shown in figure 7, this catalyst exhibited effective catalytic activity and stability, and provided over 94% of CH₄ conversion and 98% of CO selectivity, which remained almost unchanged during the entire experimentation time (100 h). No phase transformation was found, suggesting a main reason for the significantly catalytic activities and stability of NiO/BaO·6Al₂O₃ catalyst.

XPS analysis further demonstrated low tendency for carbon deposition to residual surface CO₃²⁻. Deposition of surface carbon could not be detected even when the sample was reacted under CH₄/O₂/He (40 ml/20 ml/40 ml) mixtures for 2 h at 850 °C, which further suggests that NiO/BaO·Al₂O₃ possesses excellent ability to suppress carbon deposition. Claridge *et al.* [36] clearly demonstrated that a significant amount of carbon can be formed on Ni/Al₂O₃ within a very short time (<1 h) at 1050 K. We found that the amount of

carbon deposited on the reduced NiO/BaO·Al₂O₃ after 100 h was lower than that of NiO/Al₂O₃ prepared by impregnation after 80 h of operation [37]. Vogt *et al.* [38] and Al-Ubaid and Wolf [39] have reported that the interaction between active species and the support can prevent surface carbon deposition and improve stability.

4. Conclusion

In our study, the application of barium hexaaluminate as a support material for nickel catalysts used in methane partial oxidation was successful due to its large surface area above 15 m²/g even after heating at 1200 °C. A CH₄ conversion of ~95% with CO selectivity >98% could be attained at 850 °C, and the activity and selectivity of the catalyst was unchanged after 100 h of time on stream. The “layered aluminate type” structure in the atomic arrangement in the mirror plane of the barium hexaaluminate appears to prevent decomposition of the lattice by Ni ions. The interaction between Ni ions and the support appears to suppress carbon deposition resulting in high catalyst stability.

References

- [1] D. Dissanayake, M.P. Rosynek, K.C.C. Kharas and J.H. Lunsford, *J. Catal.* 132 (1991) 117.
- [2] M. Fathi, K. Heitnes Hofstad, T. Sperle, O.A. Rokstad and A. Holmen, *Catal. Today* 42 (1998) 205.
- [3] M.A. Goula, A.A. Lemonidou, W. Grunert and M. Baerns, *Catal. Today* 32 (1996) 149.
- [4] D.A. Hickman and L.D. Schmidt, *J. Catal.* 138 (1992) 267.
- [5] R.E. Kirk and D.F. Othmer, eds., *Encyclopedia of Chemical Technology*, 3rd Ed., Vol. 12 (Wiley-Interscience, New York, 1980) p. 938.
- [6] *Ullmann's Encyclopedia of Industrial Chemistry*, 5th Rev. Ed., Vol. A12 (VCH, Weinheim, 1989) p. 169.
- [7] V.R. Choudhary, A.M. Rajput and V.H. Rane, *J. Phys. Chem.* 96 (1992) 8686.
- [8] J.R. Rostrup-Nielsen and J.H.B. Hansen, *J. Catal.* 144 (1993) 38.
- [9] R. Prasad, L.A. Kennedy and R. Ruckenstein, *Catal. Rev.* 26 (1984) 1.
- [10] M. Audier, A. Oberlin, M. Oberlin, M. Coulon and L. Bonnetain, *Carbon* 19 (1981) 217.
- [11] S.B. Tang, F.L. Qiu and S.J. Lu, *Catal. Today* 24 (1995) 253.
- [12] C.H. Bartholomew, *Stud. Surf. Sci. Catal.* 88 (1994) 1.
- [13] C.H. Bartholomew and W.L. Sorensen, *J. Catal.* 81 (1983) 131.
- [14] D.J. Young, P. Udaja and D.L. Trimm, *Catalyst Deactivation* (Elsevier, New York, 1980).
- [15] S. Blonski and S.H. Garofalim, *Catal. Lett.* 25 (1994) 325.
- [16] Z.R. Ismagilov, R.A. Shkrabina, N.A. Koryabkina and F. Kapteijn, *Catal. Today* 24 (1995) 269.
- [17] L.X. Cao, Y.X. Chen and W.Z. Li, *J. Mol. Catal. (China)* 8 (1994) 375.
- [18] V.R. Choudhary, V.H. Rane and A.M. Rajput, *Catal. Lett.* 22 (1993) 289.
- [19] C. Cristiani, P. Forzatti and P.L. Villa, *Appl. Catal. A* 104 (1993) 101.
- [20] H. Arai and M. Machida, *Appl. Catal. A* 138 (1996) 161.
- [21] M. Machida, K. Eguchi and H. Arai, *Bull. Chem. Soc. Jpn.* 61 (1988) 3659.
- [22] M. Machida, K. Eguchi and H. Arai, *J. Catal.* 103 (1987) 385.
- [23] G. Busca, *Catal. Today* 27 (1996) 323.
- [24] G. Busca, *Catal. Lett.* 31 (1995) 65.
- [25] M. Bellotto, G. Busca, C. Cristiani and G. Groppi, *J. Solid State Chem.* 117 (1995) 8.

- [26] J.M.P.J. Verstegen and A.L.N. Stevels, *J. Lumin* 9 (1974) 406.
- [27] A.L.N. Stevels and A.D.M. Schrama-de Pauw, *J. Electrochem.* 123 (1976) 691.
- [28] L. Chen, L. Lin, Z. Xu, X. Li and T. Zhang, *J. Catal.* 157 (1995) 190.
- [29] F. Basile, L. Basin and M.D. Amore, *J. Catal.* 173 (1998) 247.
- [30] L. Lietti, C. Cristiani, G. Groppi and P. Forzatti, *Catal. Today* 59 (2000) 191.
- [31] G. Groppi, M. Bellotto, C. Cristiani, P. Forzatti and P.L. Villa, *J. Mater. Sci.* 34 (1999) 1.
- [32] J.M. Rynkowski, T. Paryjczak and M. Lenik, *Appl. Catal. A* 106 (1993) 73.
- [33] P.K. De Beks, W.B.A. Wassenberg and J.W. Geus, *J. Catal.* 104 (1987) 86.
- [34] B. Scheffer, P. Molhoek and J.A. Moulijn, *Appl. Catal.* 46 (1989) 11.
- [35] C.P. Li, A. Proctor and D.M. Hercules, *Appl. Spectrosc.* 38 (1984) 880.
- [36] J.B. Claridge, M.L.H. Green, S.C. Tsang, A.P.E. York, A.T. Ashcroft and P.D. Battle, *Catal. Lett.* 22 (1993) 299.
- [37] Y.H. Zhang, Ph.D. dissertation, China (August 2000).
- [38] E.T.C. Vogt, A.J. van Dillen and J.W. Geus, *Stud. Surf. Sci. Catal.* 34 (1987) 221.
- [39] A. Al-Ubaid and E.E. Wolf, *Appl. Catal.* 40 (1988) 73.